# Detectability of damages in Carbon Fiber Reinforced Plastics using Acoustic Emission

Jonathan Liebeton<sup>1</sup> and Dirk Söffker<sup>2</sup>

<sup>1,2</sup> Chair of Dynamics and Control, University of Duisburg-Essen, Duisburg, 47057, Germany jonathan.liebeton@uni-due.de soeffker@uni-due.de

#### ABSTRACT

This contribution examines the usefulness of Acoustic Emissions (AE) as a non-destructive testing (NDT) method for detecting and distinguishing damages in carbon fiber reinforced polymer (CFRP) structures. Despite the widespread use of CFRP materials in various industries due to their favorable strength-to-weight ratio, the susceptibility to concealed internal damages necessitates advanced inspection techniques. Acoustic Emission, describing the use of ultrasonic waves emitted during deformation or damage events, is a proven and promising solution for real-time and reliable damage assessment. The study focuses on comparing two approaches: 1) a one-class Support Vector Machine (SVM) for initial damage detection, followed by detailed damage classification, and 2) a direct classification approach using five classes (four representing the material specific damage types and one for background noise). Both approaches undergo a systematic evaluation under diverse loading conditions to assess their reliability. A comprehensive experimental setup subjects CFRP specimens to controlled loading conditions, inducing various damage types and severities. Signal analysis reveals characteristic patterns associated with different damage modes, including matrix cracking, fiber breakage, debonding, and delamination. The investigation considers the influence of loading conditions on the detection and classification results to examine the robustness of the approach. The comparison between methodologies involves established metrics and analyses the posterior probability of the trained models, considering the impact of loading conditions on performance. The experimental results show AE's effectiveness in detecting and classifying damages in CFRP structures, offering insights into technique sensitivity and specificity for different damage types. These findings contribute new knowledge to the NDT field, presenting a promising path for the advancement of CFRP structural health monitoring and maintenance prac-

Jonathan Liebeton et al. This is an open-access article distributed under the terms of the Creative Commons Attribution 3.0 United States License, which permits unrestricted use, distribution, and reproduction in any medium, provided the original author and source are credited.

tices in engineering applications. The study's nuanced understanding of the strengths and limitations of the two classification approaches, considering loading conditions, contributes to the optimization of NDT strategies for diverse operation scenarios.

#### 1. Introduction

The industrial demand for carbon fiber reinforced plastics (CFRP) has been steadily increasing over the past decades, primarily due to its high strength-to-weight ratio. This characteristic makes CFRP especially advantageous in the aerospace sector, where it is used to replace heavier materials such as aluminum. Its widespread adoption is driven not only by the need to reduce fuel consumption and carbon dioxide emissions but also by the potential to extend maintenance intervals and reduce overall operational costs (Zhang, Lin, Vaidya, & Wang, 2023). In addition, CFRP plays a crucial role in meeting climate targets across sectors including automotive and renewable energy, where the material is used in components like hydrogen pressure vessels and wind turbine structures (Azeem et al., 2022; Olabi et al., 2021).

Replacing metals with CFRP introduces new challenges, particularly in monitoring and maintenance, due to the material?s non-ductile failure behavior and anisotropic structure. Traditional visual inspection methods are inadequate for CFRP, prompting the adoption of advanced Structural Health Monitoring (SHM) techniques. Among these, Acoustic Emission (AE) stands out as a passive non-destructive testing (NDT) method that enables in-situ monitoring without injecting external energy. Acoustic Emission relies on ultrasonic waves generated within the material during damage events. These waves propagate through the structure and can be detected by piezoelectric wafer active sensor (PWAS), allowing the identification and classification of damage mechanisms in real time.

The increasing complexity and remote operation of modern industrial plants, such as offshore wind farms, further emphasize the importance of reliable SHM systems. In such environments, accessibility is limited and weather-dependent, making reactive maintenance strategies costly and inefficient (Tusar & Sarker, 2022). To address this, condition-based maintenance strategies utilizing AE monitoring are developed to schedule interventions before failure occurs, thereby reducing downtime and enhancing operational efficiency (Ren, Verma, Li, Teuwen, & Jiang, 2021; Colone, Dimitrov, & Straub, 2019).

Carbon fiber reinforced plastics damage classification via AE signals commonly involves extracting features from timefrequency and frequency domains. Each type of damage, delamination, matrix crack, debonding, and fiber breakage, is associated with a characteristic frequency range, typically between 10 to 500 kHz (Baccar & Söffker, 2017). Delamination, the separation of fiber layers, is observed in the lowest frequency range, e.g., 30 to 90 kHz (Hamdi et al., 2013) and 50 to 150 kHz (Gutkin et al., 2011). This damage type is additionally characterized by the existance of the extensional and dominant flexural modes (Prosser, 1998; de Oliveira & Marques, 2008; Baccar & Söffker, 2017). Matrix cracks, which affect the resin matrix, are typically detected in the 100 to 250 kHz range (Oskouei, Heidary, Ahmadi, & Farajpur, 2012; Azadi, Sayar, Ghasemi-Ghalebahman, & Jafari, 2019), while debonding, fiber-matrix separation, occurs between 170 to 350 kHz (Marec, Thomas, & El Guerjouma, 2008; Yousefi, Ahmadi, Shahri, Oskouei, & Moghadas, 2014). A extensional with higher propagation speed and flexural modes are observed in the AE signals of matrix cracks (Johnson, 2000). Fiber breakage, the most severe form of damage, manifests at the highest frequencies, reported between 270 to 500 kHz (Chelliah, Parameswaran, Ramasamy, Vellayaraj, & Subramanian, 2019; Sayar, Azadi, Ghasemi-Ghalebahman, & Jafari, 2018; De Groot, Wijnen, & Janssen, 1995).

The absolute frequency values vary with material and loading conditions, the relative frequency order of damage mechanisms remains consistent. In Sai Krishna, Raju, and Desarkar (2024) damage mechanisms in CFRP are classified using a convolutional neural network (CNN) with features based on the short-time Fourier transform (STFT) of the related AE signals. This approach reches an accuracy of 96.9 %. Liu et al. (2023) classify the damage mechanisms matrix crack, debonding, and fiber breackage based on features derived from continuous wavelet transform (CWT) of the AE signals. The trained CNN reaches an accuracy of 96.3 %. In Barile, Casavola, Pappalettera, and Paramsamy Kannan (2022) the damage mechanisms are classified by employing a CNN in combination with features from Mel spectrograms of the acoustic waveforms. The overall accuracy for all four damage mechanisms is 97.9 %. Xue, Wang, Liang, Ma, and Zhou (2025) classifiy AE signals measured during tensile tests of fiber bundles and resin polymer. The classification of fiber breakages and matrix cracks based on the signals peak frequency reached an accuracy of 96.2 and 97.9 %. In the literature high accuracies in the classification of damage mechanisms in CFRP using data driven methods are shown, but the detection of relevant AE events is often ignored. Amplitude threshold approaches for detection are unreliable due to the exponential attenuation of ultrasonic waves in CFRP. Therefore, the detection of damage events must be considered in the classification, because only detected events can be classified. Additionally, studies show that classification accuracy is influenced by the system's operational conditions. For instance, (Rothe, Wirtz, Kampmann, Nelles, & Söffker, 2017), (Wirtz, Beganovic, & Söffker, 2016) and (Wirtz, Beganovic, & Söffker, 2019) demonstrate that AE signal classification can be affected by load-induced changes, and reliability improves through classifier fusion or probabilistic approaches.

This work presents an experimental study on AE signal detection and classification in CFRP under controlled loading conditions. The results of the detection and classification are combined for a full damage assessment. The influence of loading conditions on detection and classification reliability is investigated by analyzing the posterior probabilities. In section 2 the experimental setup, data acquisition process, and labeling strategy are introduced. In section 3 signal processing and feature extraction methods along with the machine learning-based classification approach are discussed. In section 4 detection and classification results using standard evaluation metrics are presented, while section 5 the work is concluded with a summary and outlook.

### 2. DATA SET

The experiments are divided into two main phases: the initial damage phase and the cyclic loading phase. In both phases, CFRP specimens are used, consisting of three layers arranged in a  $90^{\circ}/0^{\circ}/90^{\circ}$  orientation. The dimensions of the tested CFRP plates for cyclic loading are  $130 \times 60 \times 2$  mm. The specimens are equipped with piezoelectric sensors to detect AE signals generated during damage events.

In the initial damage phase, the CFRP specimens are damaged through indentation. The experimental procedure is described in (Wirtz et al., 2019). Compared to (Wirtz et al., 2019), the current set-up has been modified to accommodate shorter specimens, and displacement is no longer used as the control parameter due to the progressive degradation in material stiffness (Wang & Zhang, 2020). Instead, the input amplitude of the power supply is controlled to maintain constant loading conditions.

Different indentors are employed to simulate various damage mechanisms. A conical indentor with an obtuse angle and a diameter of 100 mm is used to apply bending loads, while a smaller indentor with an acute angle and a diameter of 16 mm is used to directly damage the matrix, simulating impact-type damage (Baccar & Söffker, 2017). The CFRP specimens are fixed using a clamping system to ensure repeatability during

the indentation procedure. Depending on the indentor shape and size, different damage mechanisms are induced.

Additionally, two- and three-point bending tests are conducted. For these procedures, the CFRP specimens are fixed at two or three support points, respectively, and bent until full material failure occurs. These methods further diversify the types of damage mechanisms captured during testing.

In the cyclic loading phase, previously damaged specimens are clamped between a stationary bench vise and a slider. The test rig shown in figure 1 converts a voltage sine signal into a proportional current signal using a power supply, ensuring constant excitation force (Liebeton, Soon, & Söffker, 2023). Frequencies and amplitudes range from 2 to 6 Hz and 2 to 6 V, respectively. A crank mechanism converts rotary motion into translatory motion to cyclically bend the specimen. Displacement of the slider is monitored by a proximity sensor, with measured values between 6 to 10 mm.

In both static and cyclic experiments, AEs are recorded continuously from the undamaged state through to full material failure. PWASs, each with a diameter of 10 mm and a thickness of 1 mm, are bonded to the surface of the specimens. These sensors transform mechanical stress waves into analog electrical signals via the piezoelectric effect. The analog signals are pre-amplified with high input impedance and low output impedance to preserve signal quality, then digitized by a field programmable gate array (FPGA) board with a 4 MHz sampling frequency and 16-bit resolution (Dettmann, 2012).

The AE data are manually labeled based on literaturedescribed waveform and frequency content. Signal sections containing no AE events are labeled as noise. This approach enables the development of a detailed and mechanismspecific AE data set.

### 3. METHODS

The raw AE measurement data are processed using a multistage signal processing and classification pipeline to extract features and assign them to specific damage mechanisms. The AE signals are continuously recorded and divided into segments of  $2^{10}$  samples. To mitigate frequency artifacts caused by signal segmentation, a half Hamming window is applied to the first and last  $2^5$  samples of each segment.

Relevant AE events are first detected through signal energy analysis in the frequency range of 10 to 500 kHz. This is achieved by computing the STFT of the measurement data. The STFT of a signal x(t) is defined as

$$X_F(\omega, \tau) = \int_{-\infty}^{\infty} x(t)\gamma(t - \tau)e^{-j\omega t}dt, \qquad (1)$$

where  $\gamma(t-\tau)$  denotes the window function applied at time  $\tau$ . The resulting spectral coefficients are used to compute the

signal energy over time. Thresholding is applied to identify segments with high energy content in the defined frequency range. These segments are manually analyzed and labeled based on the known characteristics of AE signals for various damage mechanisms.

Each identified AE event segment is transformed into two distinct sets of features. One is based on the fast Fourier transform (FFT), the other on the CWT. For both methods, only the frequency range of 10 to  $500~\mathrm{kHz}$  is considered.

The FFT transforms the time-domain signal x(n) into the frequency domain and is defined as

$$X_F(k) = \sum_{n=0}^{N-1} x(n)e^{-j\omega_k n},$$
 (2)

with 
$$\omega_k = 2\pi k/N$$
,  $k = 0, 1, ..., N - 1$ .

The resulting FFT-based feature vector consists of 126 features describing the frequency behavior within the relevant frequency band.

The CWT is defined as

$$X_W(s,\tau) = \frac{1}{\sqrt{s}} \int_{-\infty}^{\infty} x(t) \Psi^* \left(\frac{t-\tau}{s}\right) dt, \qquad (3)$$

where  $\Psi^*$  is the complex conjugate of the wavelet function, s is the frequency scale, and  $\tau$  is the translation in time. The CWT provides a time-scale representation of the signal, offering high frequency resolution at large scales and high time resolution at small scales. The CWT-based feature vector is derived from the column of the coefficient matrix with the maximum overall value. The resulting vector contains 53 elements.

The detection and classification of AE events are realized through variations of SVM. The classical support vector machine (SVM) is a binary supervised classifier that finds a hyperplane to separate two classes. The objective of the training process is to maximize the margin between the hyperplane and the support vectors, the data points closest to the decision boundary. If data are not linearly separable, kernel functions are employed to project the data into a higher-dimensional space where linear separation is feasible. Slack variables can be introduced to create soft-margin SVMs, enabling tolerance for misclassifications and mitigating overfitting. Strategies for extending SVMs to multi-class problems are used. In the one against all (OAA) approach each class is compared against all others, resulting in  $N_{OAA} = C$  classifiers for Cclasses. The class with the highest decision value is selected. The one against one (OAO): Every pair of classes is compared, requiring  $N_{OAO}=\frac{C(C-1)}{2}$  classifiers. The final class decision is based on majority voting across all binary classifiers.

For probabilistic classification, the decision value f of each



Figure 1. Experimental set-up for cyclic loading, Chair Dynamics and Control, U DuE, Germany

SVM is transformed into a posterior probability  $r_{ij}$  using

$$r_{ij} = \frac{1}{1 + e^{Af + B}},$$
 (4)

where A and B are parameters estimated by minimizing the negative log likelihood of the training data ((Chang & Lin, 2011; Platt, 1999)). The overall class probabilities  $p_i$  are computed by solving the quadratic program proposed by (Wu, Lin, & Weng, 2004)

$$\min_{p} \frac{1}{2} \sum_{i=1}^{N} \sum_{j:j \neq i} (r_{ji} p_i - r_{ij} p_j)^2, \tag{5}$$

where 
$$p_i \ge 0, \forall i$$
, and  $\sum_{i=1}^{N} p_i = 1$ .

In addition to supervised classification, an unsupervised one class support vector machine (1C-SVM) is used and trained only on a single class of data. The algorithms learns the boundary that encompasses the majority class. Points far from the decision boundary, particularly those close to the origin, are considered anomalies. Kernel transformations are also applicable in the one-class setting.

This contribution evaluates two approaches for AE signal detection and classification, which are initially introduced in (Liebeton & Söffker, 2025). The general framework is shown in figure 2. The first approach is a direct distinction between the four damage classes and noise. Detection and classification is done in one step using a five class support vector machine (5C-SVM). In the second approach a 1C-SVM is first

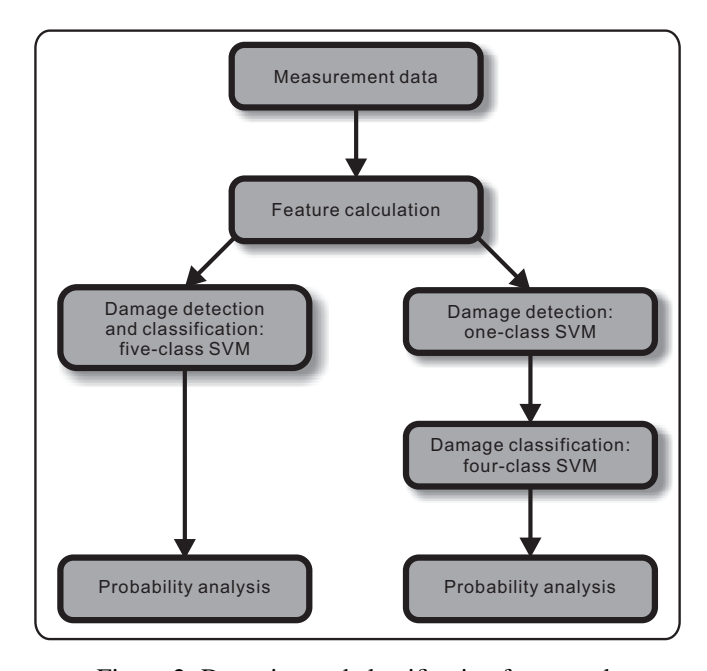


Figure 2. Detection and classification framework

used to separate noise from relevant AE signals. The nonnoise signals are then classified into one of the four damage types using a four class support vector machine (4C-SVM). Both approaches are trained and tested using CWT- and FFTbased features. To enhance generalization and prevent overfitting, 10-fold cross-validation is applied. Each damage class includes 390 labeled samples, of which 260 samples are used for training and the remaining 130 samples are used for test-

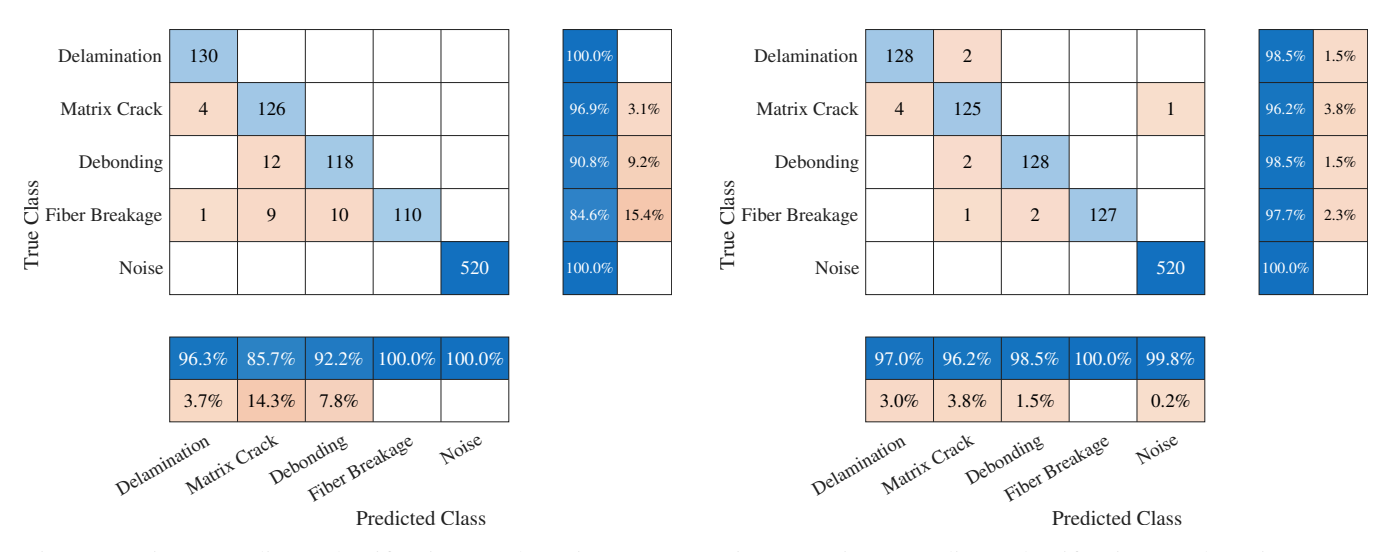


Figure 3. 5C-SVM direct classification results using FFTbased features

ing. The noise class consists of 1040 samples for training and 520 samples for testing.

## 4. RESULTS

The two approaches and the two sets of features are evaluated based on their combined performance in detection and classification of AE events.

The direct classification results of the 5C-SVM using FFT-based features are shown in figure 3. The model is using the OAA approach to combine the single SVM model. The SVMs use a linear kernel and a regularization parameter of 0.0101. The model has perfect detection results as all noise and damage events are correctly separated, but for the damage class fiber breakage an accuracy of 84.6 % is achieved. The best results of this approach is reached for the damage class delamination. The combined accuracy for the detection and classification is 96.5 %.

In figure 4 the direct classification results of the 5C-SVM using CWT-based features are shown. The OAA strategy is employed to combine multiple SVM classifiers. Each SVM applies a linear kernel and uses a regularization parameter set to 0.0024. In direct comparison with the FFT-based features using the same approach, the CWT-based features reach higher accuracies. One damage event is not being detected, but all events containing noise are correctly classified. The lowest accuracy with 96.2% is obtained for the classification of matrix cracks and the highest with 98.5% for the two classes delamination and debonding. With an overall accuracy of 98.8% the CWT-based features outperform the FFT-based features in the direct classification apporach.

The combined results of the 1C-SVM detection and 4C-SVM classification of detected events using FFT-based features are

Figure 4. 5C-SVM direct classification results using CWT-based features

shown in figure 5. The 4C-SVM classifier uses the OAA method. Each SVM has a linear kernel with a regularization parameter of 0.1096. The separated detection and classification approach using FFT-based features is performing better than the direct classification approach. The detection accuracy is 100~%. The lowest accuracy with 86.9~% is obtained for the damage class fiber breakage. The combined accuracy is 97.4~%.

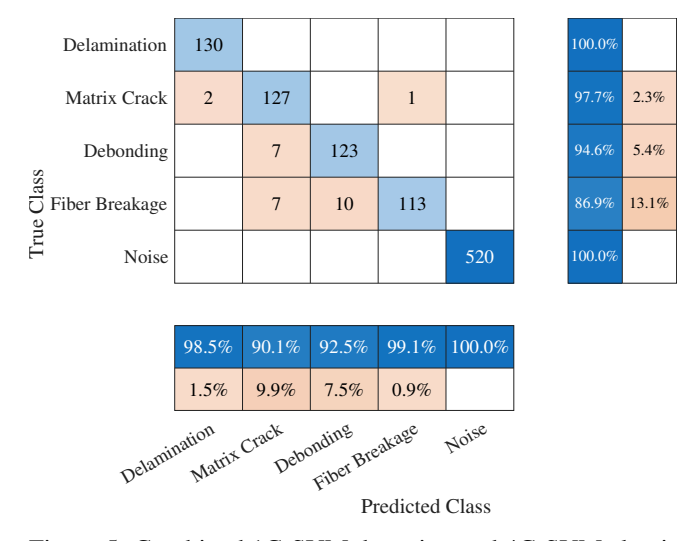


Figure 5. Combined 1C-SVM detection and 4C-SVM classification results using FFT-based features

In figure 6 the combined results of the 1C-SVM detection and 4C-SVM classification of detected events using CWT-based features are shown. The trained 4C-SVM classifier is using the OAA method. Each SVM employs a linear kernel with a regularization parameter of 0.0060. The detection of damage events and classification of delaminations is performed with an accuracy of 100 %. In total only seven missclassi-

fications are observed for the classes matrix crack, debonding, and fiber breakage. For the combined 1C-SVM detection and 4C-SVM classification using CWT-based features the highest overall accuracy is achieve with 99.3 %. Neglecting the detection, the classification accuracy is 98.6 %, which ist slightly higher than the reported results in the literature.

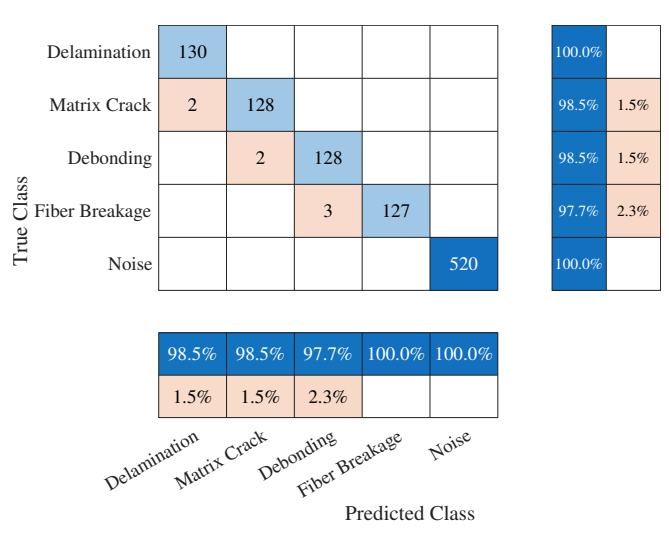


Figure 6. Combined 1C-SVM detection and 4C-SVM classification results using CWT-based features

Both approaches and sets of features are able to successfully separate damage events from noise, only in the case of directly classifying AE signals based on CWT features one damage event is not detected. An increased number of Fiber breakage missclassifications can be observed using FFT-based features. The AE signature of fiber breakage events is generally in the range of  $10~\mu s$  and the evaluated time window has a length of  $256~\mu s$ . Therefore, the FFT is not always able to filter the required information of highly transient signals, but contains information of the entire window duration enabling detection of multiple damage events within the windowed signal. The two stage approach of detection and classification outperforms the direct classification approach and the CWT-based features lead in both approaches to better results than using only features from FFT analysis.

The evaluation of probability estimations with respect to the loading conditions is performed for each damage mechanism. Because of the better performance of the CWT-based features, only the probability estimations of the separated detection and classification approach and the direct classification approach using CWT-based features are presented. In the case of multiple damage mechanisms of the same class being detected at the same excitation frequency and excitation voltage combination, the average probability estimation is calculated. If no damage is detectable at a specific combination of excitation frequency and excitation voltage, the probability estimation is zero.

In figure 7 the probability estimations depending on frequency and input voltage for 5C-SVM direct classification results using CWT-based features are visualized by the color code. In the range of 1 to 2 V and 2 Hz, and starting from 3 V and 6 Hz to 4.5 V and 2 Hz no delaminations are detectable. In the enclosed region delaminations are detected with high probabilities. In the range of 2 to 2.5 V and 2.5 to 3.5 Hz matrix cracks are detected with a probability of 60 %. The surrounding regions in the range of 1.5 to 4.5 V and 2 to 6 Hz the probability is at 100 %. Debonding is detected at 2 Hz in the range of 2 to 5 V, at 3 Hz and 3 V, 5 Hz and 2.5 V, and 3 Hz and 1 V. Fiber Breakages are detectable in the range of 1.5 to 4 V and 2.5 to 6 Hz, at 3 Hz and 5 V, and 2 Hz and 5.5 V.

The probability estimations depending on frequency and input voltage for combined 1C-SVM detection and 4C-SVM classification results using CWT-based features are shown in figure 8. The only difference in the detection of delaminations can be observed at 2.5 Hz and 2 V, where the separated detection and classification approach shows higher probabilities. Differences in matrix crack detection are observable in the range of 2 to 2.5 V and 2.5 to 3.5 Hz, where the direct classification approach shows a lower probability.

The high accuracy of the chosen models lead to high probability estimations in specific ranges of excitation frequencies and excitation voltages. The combinations of excitation frequencies and excitation voltages with probability estimations of zero indicate that under certain loading conditions damages are not detectable.

#### 5. CONCLUSIONS AND OUTLOOK

The comparison of direct classification and separated detection and classification in combination with FFT- and CWT-based features shows, the chosen CWT-based features in combination with separated detection and classification outperforms the direct classification approach and FFT-based features. The highest overall accuracy is achieved for the combined 1C-SVM detection and 4C-SVM classification using CWT-based features with 99.3 %. The evaluation of probability estimations show a dependency between detection and classification performance and loading conditions.

In future works an online detection and classification loop can be established which switches between detection and classification models based on their performance at the given loading conditions. Additionally the occurrence of multiple damage mechanisms at the same time are to be investigated to further improve monitoring reliability.

# REFERENCES

Azadi, M., Sayar, H., Ghasemi-Ghalebahman, A., & Jafari, S. M. (2019). Tensile loading rate effect on mechanical

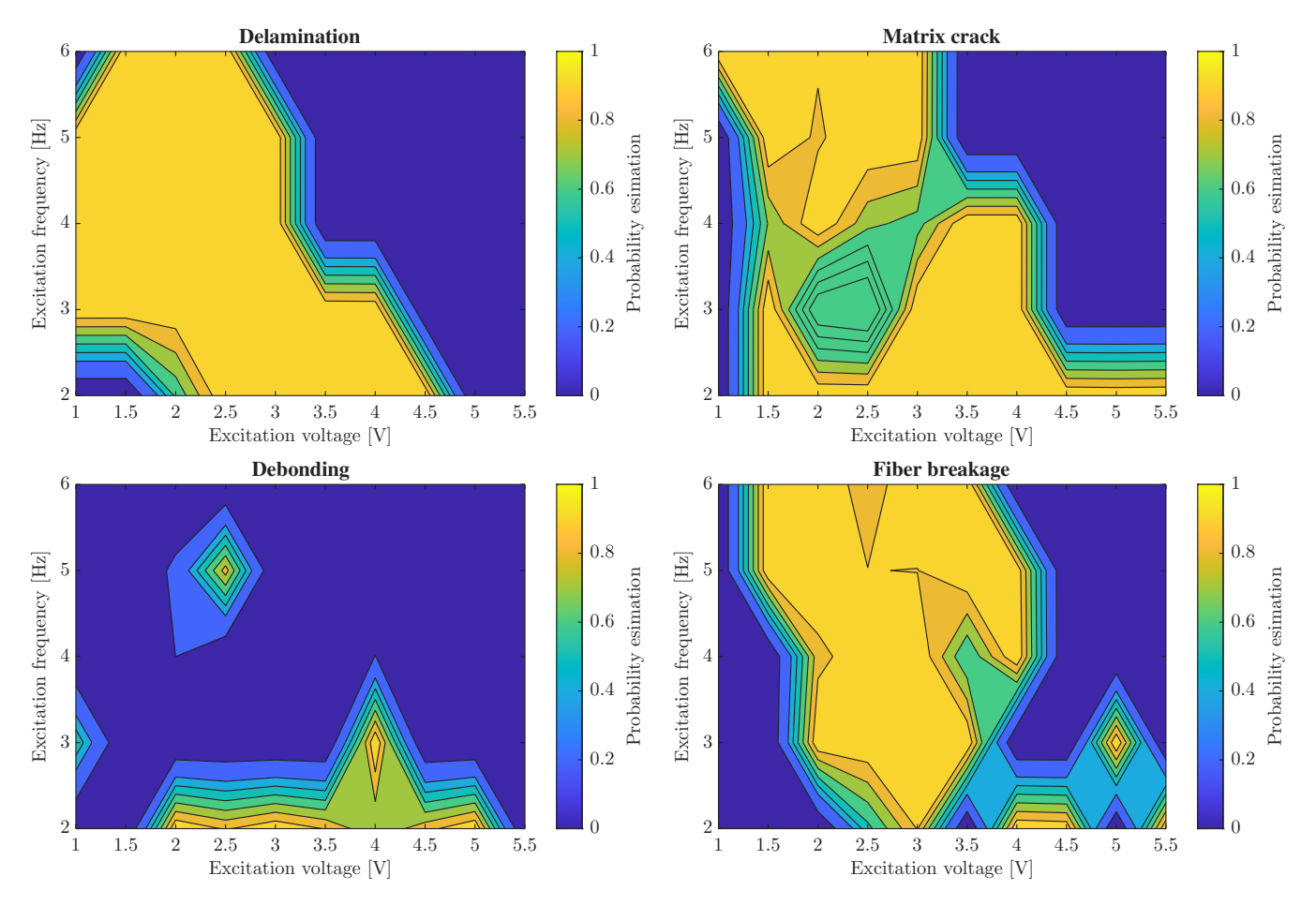


Figure 7. Probability estimations depending on frequency and input voltage for 5C-SVM direct classification results using CWT-based features

properties and failure mechanisms in open-hole carbon fiber reinforced polymer composites by acoustic emission approach. *Composites Part B: Engineering*, 158, 448–458.

Azeem, M., Ya, H. H., Alam, M. A., Kumar, M., Stabla, P., Smolnicki, M., ... Mustapha, M. (2022). Application of filament winding technology in composite pressure vessels and challenges: A review. *Journal of Energy Storage*, 49, 1–22.

Baccar, D., & Söffker, D. (2017). Identification and classification of failure modes in laminated composites by using a multivariate statistical analysis of wavelet coefficients. *Mechanical Systems and Signal Processing*, 96, 77–87. doi: 10.1016/j.ymssp.2017.03.047

Barile, C., Casavola, C., Pappalettera, G., & Paramsamy Kannan, V. (2022). Damage monitoring of carbon fibre reinforced polymer composites using acoustic emission technique and deep learning. *Composite Structures*, 292, 115629. doi: 10.1016/j.compstruct.2022.115629

Chang, C.-C., & Lin, C.-J. (2011). Libsvm: A library for support vector machines. *ACM Transactions on* 

*Intelligent Systems and Technology*, 2(3), 1–27. doi: 10.1145/1961189.1961199

Chelliah, S. K., Parameswaran, P., Ramasamy, S., Vellayaraj, A., & Subramanian, S. (2019). Optimization of acoustic emission parameters to discriminate failure modes in glass–epoxy composite laminates using pattern recognition. *Structural Health Monitoring*, 18(4), 1253–1267.

Colone, L., Dimitrov, N., & Straub, D. (2019). Predictive repair scheduling of wind turbine drive—train components based on machine learning. *Wind Energy*, 22(9), 1230–1242. doi: 10.1002/we.2352

De Groot, P. J., Wijnen, P. A., & Janssen, R. B. (1995). Real-time frequency determination of acoustic emission for different fracture mechanisms in carbon/epoxy composites. *Composites science and technology*, 55(4), 405–412.

de Oliveira, R., & Marques, A. T. (2008). Health monitoring of frp using acoustic emission and artificial neural networks. *Computers & Structures*, 86(3-5), 367–373. doi: 10.1016/j.compstruc.2007.02.015

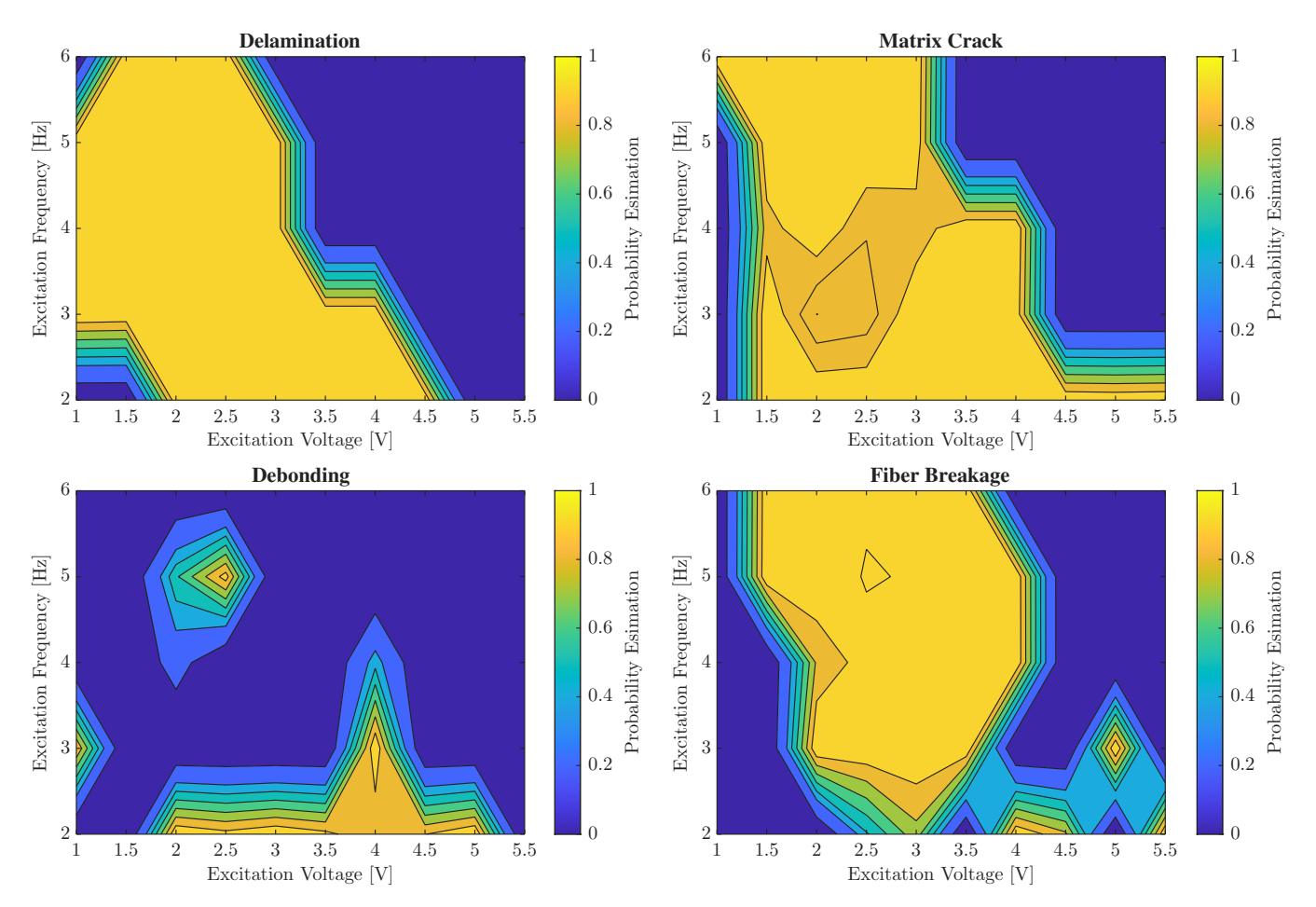


Figure 8. Probability estimations depending on frequency and input voltage for combined 1C-SVM detection and 4C-SVM classification results using CWT-based features

Dettmann, K.-U. (2012). Probabilistic-based method for realizing safe and reliable mechatronic systems. (Dr.-Ing. dissertation, University of Duisburg-Essen, Germany)

Gutkin, R., Green, C., Vangrattanachai, S., Pinho, S., Robinson, P., & Curtis, P. (2011). On acoustic emission for failure investigation in cfrp: Pattern recognition and peak frequency analyses. *Mechanical Systems and Signal Processing*, 25(4), 1393-1407. doi: https://doi.org/10.1016/j.ymssp.2010.11.014

Hamdi, S. E., Le Duff, A., Simon, L., Plantier, G., Sourice, A., & Feuilloy, M. (2013). Acoustic emission pattern recognition approach based on hilbert–huang transform for structural health monitoring in polymer-composite materials. *Applied Acoustics*, 74(5), 746–757.

Johnson, M. (2000). Broad-band transient recording and characterization of acoustic emission events in composite laminates. *Composites Science and Tech*nology, 60(15), 2803–2818. doi: 10.1016/S0266-3538(00)00148-2

Liebeton, J., & Söffker, D. (2025). Damage detection in cfrp using acoustic emission. *Proceedings of the XX Inter*-

national Symposium on Dynamic Problems of Mechanics. doi: 10.26678/ABCM.DINAME2025.DIN2025-0069

Liebeton, J., Soon, S. M. S., & Söffker, D. (2023). Improving the diagnostic reliability of ae-based failure mode detection and distinction in cfrp. In M. P. Brito, T. Aven, P. Baraldi, M. Čepin, & E. Zio (Eds.), *Proceedings of the 33rd european safety and reliability conference (esrel 2023)* (pp. 1298–1304). Research Publishing, Singapore. doi: 10.3850/978-981-18-8071-1\_P176-cd

Liu, Y., Huang, K., Wang, Z.-x., Li, Z., Chen, L., Shi, Q., ... Guo, L. (2023). Cross-scale data-based damage identification of cfrp laminates using acoustic emission and deep learning. *Engineering Fracture Mechanics*, 294, 109724. doi: 10.1016/j.engfracmech.2023.109724

Marec, A., Thomas, J.-H., & El Guerjouma, R. (2008). Damage characterization of polymer-based composite materials: Multivariable analysis and wavelet transform for clustering acoustic emission data. *Mechanical systems and signal processing*, 22(6), 1441–1464.

Olabi, A. G., Wilberforce, T., Elsaid, K., Sayed, E. T.,

- Salameh, T., Abdelkareem, M. A., & Baroutaji, A. (2021). A review on failure modes of wind turbine components. *Energies*, 14(17), 1–44.
- Oskouei, A. R., Heidary, H., Ahmadi, M., & Farajpur, M. (2012). Unsupervised acoustic emission data clustering for the analysis of damage mechanisms in glass/polyester composites. *Materials & Design*, 37, 416–422.
- Platt, J. (1999). Probabilistic outputs for support vector machines and comparisons to regularized likelihood methods. *Advances in large margin classifiers*, 10(3), 61–74.
- Prosser, W. H. (1998). Wafeform analysis of ae in composites. *Proceedings of the sixth international symposium on acoustic emission from composite materials*.
- Ren, Z., Verma, A. S., Li, Y., Teuwen, J. J., & Jiang, Z. (2021). Offshore wind turbine operations and maintenance: A state-of-the-art review. *Renewable* and Sustainable Energy Reviews, 144, 110886. doi: 10.1016/j.rser.2021.110886
- Rothe, S., Wirtz, S. F., Kampmann, G., Nelles, O., & Söffker, D. (2017). Ensuring the reliability of damage detection in composites by fusion of differently classified acoustic emission measurements. *Structural Health Monitoring* 2017, 1380–1387. doi: 10.12783/shm2017/14010
- Sai Krishna, Y., Raju, G., & Desarkar, M. S. (2024). Damage mode classification in cfrp laminates using convolutional autoencoder and convolutional neural network on acoustic emission waveforms. Structural Health Monitoring. doi: 10.1177/14759217241298403
- Sayar, H., Azadi, M., Ghasemi-Ghalebahman, A., & Jafari, S. M. (2018). Clustering effect on damage mechanisms in open-hole laminated carbon/epoxy composite under constant tensile loading rate, using acoustic emission. *Composite Structures*, 204, 1–11.
- Tusar, M. I. H., & Sarker, B. R. (2022). Maintenance cost minimization models for offshore wind farms:

- A systematic and critical review. *International Journal of Energy Research*, 46(4), 3739–3765. doi: 10.1002/er.7425
- Wang, C., & Zhang, J. (2020). Experimental and analytical study on residual stiffness/strength of cfrp tendons under cyclic loading. *Materials*, 13(24), 5653. doi: 10.3390/ma13245653
- Wirtz, S. F., Beganovic, N., & Söffker, D. (2016). Experimental results of frequency-based classification of damages in composites. *8th European Workshop on Structural Health Monitoring*, *21*(8), 1–10.
- Wirtz, S. F., Beganovic, N., & Söffker, D. (2019). Investigation of damage detectability in composites using frequency-based classification of acoustic emission measurements. *Structural Health Monitoring*, *18*(4), 1207–1218. doi: 10.1177/1475921718791894
- Wu, T.-f., Lin, C.-J., & Weng, R. (2004). Probability estimates for multi-class classification by pairwise coupling. *Journal of Machine Learning Research*, 5, 975–1005.
- Xue, S.-N., Wang, J., Liang, Y.-Z., Ma, L.-H., & Zhou, W. (2025). Indentation damage identification of carbon fiber composite laminates based on modal acoustic emission and machine learning. *Polymer Composites*, 46(8), 6944–6955. doi: 10.1002/pc.29405
- Yousefi, J., Ahmadi, M., Shahri, M. N., Oskouei, A. R., & Moghadas, F. J. (2014). Damage categorization of glass/epoxy composite material under mode ii delamination using acoustic emission data: a clustering approach to elucidate wavelet transformation analysis. *Arabian Journal for Science and Engineering*, 39, 1325–1335.
- Zhang, J., Lin, G., Vaidya, U., & Wang, H. (2023). Past, present and future prospective of global carbon fibre composite developments and applications. *Composites Part B: Engineering*, 250, 1–19.